Journal of Power Sources 211 (2012) 40–45

Contents lists available at SciVerse ScienceDirect

Journal of Power Sources

journal homepage: www.elsevier.com/locate/jpowsour

In situ synthesis of polyaniline/sodium carboxymethyl cellulose nanorods for high-performance redox supercapacitors

Hui Peng, Guofu Ma*, Wenmei Ying, Aidi Wang, Haohao Huang, Ziqiang Lei*

Key Laboratory of Eco-Environment-Related Polymer Materials of Ministry of Education, Key Laboratory of Polymer Materials of Gansu Province, College of Chemistry and Chemical Engineering, Northwest Normal University, 967 Anning East Road, Lanzhou 730070, China

ARTICLE INFO

Article history:
Received 22 November 2011
Received in revised form
1 March 2012
Accepted 16 March 2012
Available online 11 April 2012

Keywords:
Polyaniline
Sodium carboxymethyl cellulose
Nanorods
Supercapacitors

ABSTRACT

Polyaniline/sodium carboxymethyl cellulose (PANI/CMC) nanorods have been synthesized via in-situ oxidation polymerization of aniline in the presence of sodium carboxymethyl cellulose as a polymerization template. The structure and morphology of the nanorods are characterized by TEM, FE-SEM and XRD. The size and shape of the composite nanorods are uniform with a diameter of 100 nm. Their electrochemical properties are also investigated using cyclic voltammetry and galvanostatic charge/discharge measurement. The specific capacitance of PANI/CMC nanorods prepared with 20 wt% CMC can be as high as 451.25 F g^{-1}. Its capacitance remains higher than 300 F g^{-1} after 1000 cycles at a current density of 1 A g^{-1}. These novel nanorods are desirable for applications in supercapacitor devides.

1. Introduction

Supercapacitors have been extensively studied as one type of the most promising candidates for next generation energy storage systems [1]. Compared with electrostatic supercapacitors or batteries, electrochemistry supercapacitors have several advantages, such as a large specific capacitance, a high power density, a long cycle life and rapid charging-discharging rates [2]. In addition, materials used in electrochemistry supercapacitor are often non-toxic and safe, while many types of batteries, e.g. nickel-cademium batteries, are toxic.

Material for electrochemistry supercapacitors recently employed can be divided into three types: (1) metal oxides or metal hydroxides [3–5], (2) conducting polymers [6], and (3) carbon materials [7,8]. Among them, noble metal oxides such as RuO_2 and conducting polymers have shown a capacity to deliver higher specific capacitance than carbon materials, since they store charges through both double-layer and redox capacitive mechanisms [9]. However, due to the low abundance and the high cost of RuO_2, conducting polymers have attracted more intensive interests as alternative materials for electrochemical energy storage applications and they exhibit a continuous range of oxidation states with increasing electrode potential [10].

Polyaniline (PANI) is generally considered suitable for the next generation of supercapacitors because of its high energy density, low cost, environmental friendliness and easy synthesis [11,12]. However, it has a relatively poor cycling stability and temperature dependence [13]. Therefore, it is often hybridized with inorganic materials (carbon materials, metal oxides or hydroxides) to prepare a composite to be used in the supercapacitors with an improved conductivity, better cycleability, specific capacitance and mechanical stability [14]. Mujawar and Lee [15] prepared a composite via electropolymerization of polyaniline on TiO_2 nanotubes, which had a specific capacitance of 740 F g^{-1} and a 13% loss over 1100 cycles. Feng et al. [16] obtained a graphene/polyaniline composite film used as the supercapacitor electrode with a specific capacitance of 640 F g^{-1} and a retention life of 90% after 1000 charge/discharge cycles. Snook et al. [17] suggested that one significant drawback of some materials is the relatively low power due to the slow diffusion of ions within the bulk of the electrode. If the dimension of the electrode materials becomes smaller, the diffusion of ions in the electrode is accelerated to improve electrochemical properties of these electrode materials. In recent years, polyaniline was template-sysnthesized in order to reduce its dimension. Xing et al. [18] reported the synthesis of polyaniline in the reversed micelles of CTAB as a surfactant. Zhou et al. [19] synthesized PANI nanofibers with high electrical conductivity using the CTAB-SDBS binary surfactants as a soft templates and a dispersion reagent. Li et al. [20] synthesized porous and mat-like polyaniline/sodium alginate nanostructured composite with good electrochemical properties in an aqueous solution with sodium alginate as a template.

* Corresponding authors. Tel./fax: +86 931 7970359.
E-mail addresses: magf@nwnu.edu.cn (G. Ma), leizq@nwnu.edu.cn (Z. Lei).

0378-7753/$ – see front matter © 2012 Elsevier B.V. All rights reserved.
doi:10.1016/j.jpowsour.2012.03.074

Sodium carboxymethyl cellulose (CMC) is polysaccharide composing the fibrous tissue of plants. Because hydroxyl groups on 2-glucopyranose residue of cellulose are replaced by carboxymethyl groups, CMC has a number of sodium carboxymethyl groups ($-CH_2COONa$) and dissolves in water. CMC is commonly employed in food processing, flocculation, drag reduction, detergents, textiles and drugs [21]. Recently, CMC is successfully used as an effective stabilizer in preparing nanoparticles, such as Ag nanoparticles [22]. α-Fe_2O_3 electrodes with CMC binder show excellent cycling performances [23]. He et al. [24] employed CMC as pre-agglomeration stabilizers and obtained highly dispersed zero valent iron nanoparticles. Among all polysaccharides, CMC is available easily and it is also affordable and environmentally friendly.

In the present paper, we used one step in-situ oxidation polymerization method to prepare polyaniline/sodium carboxymethyl cellulose nanorods using rod-like CMC as a polymerization template. The composite nanorods have a uniform diameter of 100 nm. The nanorods showed an enhanced specific capacitance and excellent cycling stability.

2. Experimental

2.1. Materials

Aniline monomer (Shanghai Chemical Works, China) was distilled under reduced pressure. Sodium carboxymethyl cellulose (CMC, Tianjing Yuanli Chemical Co., China), ammonium persulfate (APS, Tianjing Damao Chemical Co., China) were used as received. All solutions were prepared in deionized water. All Other chemical reagents were in analytical grade.

2.2. Synthesis of polyaniline/sodium carboxymethyl cellulose nanorods

Polyaniline/sodium carboxymethyl cellulose nanorod was synthesized as follows: 0.1 g sodium carboxymethyl cellulose was dissolved in 30 ml deionized water at ambient temperature. 0.4 g aniline monomer and 10 ml 1 M HCl solution were introduced into the above solution, and then the mixture was sonicated for 15 min to facilitate the adsorption of aniline onto the sodium carboxymethyl cellulose. 1.25 g $(NH_4)_2S_2O_8$ in 10 ml deionized water was added into the above system after being stirred for 30 min. The polymerization was performed for at least 12 h at room temperature. Reaction product was collected by centrifugation and washed successively with deionized water and ethanol until the filtrate was colourless, and then dried at 60 °C for 24 h in vacuum to obtain a dark green powder.

For comparison purpose, pure polyaniline without sodium carboxymethyl cellulose was also synthesized under the same conditions.

2.3. Characterizations

X-ray diffraction (XRD) of samples was performed on a diffractometer (D/Max-2400, Rigaku) using Cu Kα radiation ($k = 1.5418$ Å) at 40 kV, 100 mA. The 2θ range used in the measurements was from 5 to 80°. Morphology of the pure PANI and PANI/CMC nanorods was examined with field emission scanning electron microscopy (FESEM, JSM-6701F, Japan) at an accelerating voltage of 5.0 kV. The structure of the samples was characterized by a transmission electron microscopy (TEM, JEM-2010 Japan). FT-IR spectra were recorded on a Nicolet Nexus 670 Fourier transform infrared spectrometer using KBr tabletting technique and the spectra was in the range of 4000 - 400 cm^{-1}.

2.4. Electrochemical measurements

A typical three-electrode test cells in electrolyte was used for electrochemical measurement on the electrochemical working station (CHI650D, Chenghua, Shanghai China). All the measurements were carried out in 1 M H_2SO_4 electrolyte at room temperature. The glassy carbon electrode with a diameter of 3 mm was used as the working electrode. Platinum electrode served as the counter electrode and saturated calomel electrode (SCE) as the reference electrode. The fabrication of the working electrodes refers to Ref. [20]. Typically, 4 mg of PANI/CMC was ultrasonically dispersed in 1 mL of deionized water, and 10 μL of the polytetrafluoroethylene (PTFE) emulsion (60 wt%) was added to this dispersion. 3 μL of the above suspension was dropped onto the glassy carbon electrode using a pipet gun and dried at room temperature.

Cyclic voltammograms were recorded from −0.2 to 0.8 V at scan rates of 10, 20, 30, 50 and 80 mV s^{-1}. The measurements of the galvanostatic charge/discharge property and cycle-life stability were performed with a computer controlled cycling equipment (LAND CT2001A, Wuhan China). The galvanostatic charge/discharge property was measured at the current densities of 1, 2, 3, 5, and 10 A g^{-1} with cutoff voltage of 0−0.8 V.

3. Results and discussions

3.1. Mechanism of the formation of the nanorod structure

The one-pot synthesis of PANI/CMC composites was conducted through in-situ oxidation polymerization, as described in Scheme 1. Since sodium carboxymethyl cellulose hydrolyses in strongly acidic condition, it can be completely dissolved at room temperature. Therefore, HCl solution of low concentration was rapidly added into sodium carboxymethyl cellulose solution immediately after the addition of aniline monomer. The addition of HCl solution into the CMC solution promotes the dissociation of neutral −COONa into negatively charged $-COO^-$. As a result, the negatively charged CMC chains easily adsorb $-NH_2$ groups of anline monomer via an electrostatic interaction to form biopolymer−monomer complexes [13]. This operation will keep the structure of sodium carboxymethyl cellulose intact during hydrolysis but promote the dissociation of −COONa to $-COO^-$. Furthermore, it was observed that the electrical conductivity of polyaniline synthesized in acidic conditions is better than that obtained in basic or neutral conditions [25].

After the oxidant ammonium persulfate was introduced into the system, polyaniline was synthesized and it was attached onto the surface of sodium carboxymethyl cellulose. As a result, the PANI/CMC composite was thus prepared. CMC not only serves as a dopant for PANI but also acts as a polymerization template during the polymerization.

3.2. Morphology

Fig. 1 shows the typical morphology of the pure PANI and PANI/CMC products. One can see that pure PANI particles (Fig. 1a) aggregate into lumps with diameters ranging from 200 nm to a few microns. Their surfaces are very rough because aniline polymerization is a multi-level growth process. However, as shown in Fig. 1b, the PANI/CMC particles are of a uniform rod-like structure with a diameter of 100 nm, and a random netlike structure rather than the dense accumulation is observed in lower magnification (Fig. 1c). The PANI/CMC products structure was further characterized by transmission electron microscopy (TEM). As shown in Fig. 1d, the rod-like structure of PANI/CMC products can be clearly visible.

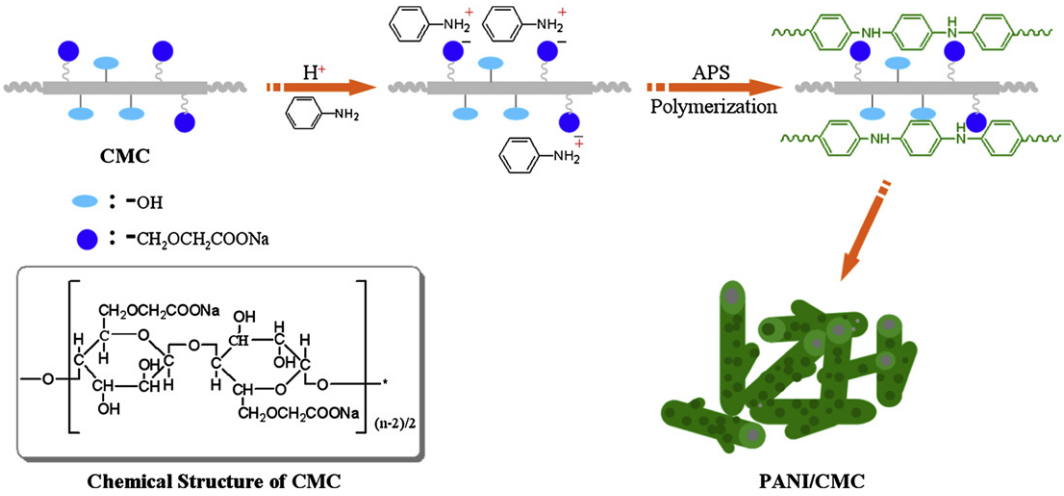

Scheme 1. Schematic of the preparation process of PANI/CMC nanocomposites.

The XRD patterns of CMC, pure PANI and PANI/CMC nanorods are compared in Fig. 2. It can be seen that diffraction of CMC shows a typical peak at 20.2°. The pure PANI has a primary characteristic peak at 25.2° attributed to the scattering from the periodicity perpendicular to PANI chains and the one at 20.3° to the alternating distance between layers of polymer chains [26]. The diffraction peak of PANI/CMC composite is similar to pure PANI, and no obvious diffraction peak at about 20° of CMC appears, since the content of CMC in the composite is very small and the CMC is uniformly dispersed in the composite materials [27].

FT–IR spectra for CMC, pure PANI, and PANI/CMC are presented in Fig. 3. The peak at 3442 cm^{-1} of CMC is due to O–H stretching vibrations, the ones at 2931 and 2871 cm^{-1} to aliphatic C–H stretching vibrations, the ones at 1620 and 1423 cm^{-1} to the asymmetric and symmetric stretching of the carboxylate group ($-COO^-$), and that at 1057 cm^{-1} to C–O–C stretching vibrations. Pure PANI has the characteristic peaks at 1576 cm^{-1} and 1485 cm^{-1}

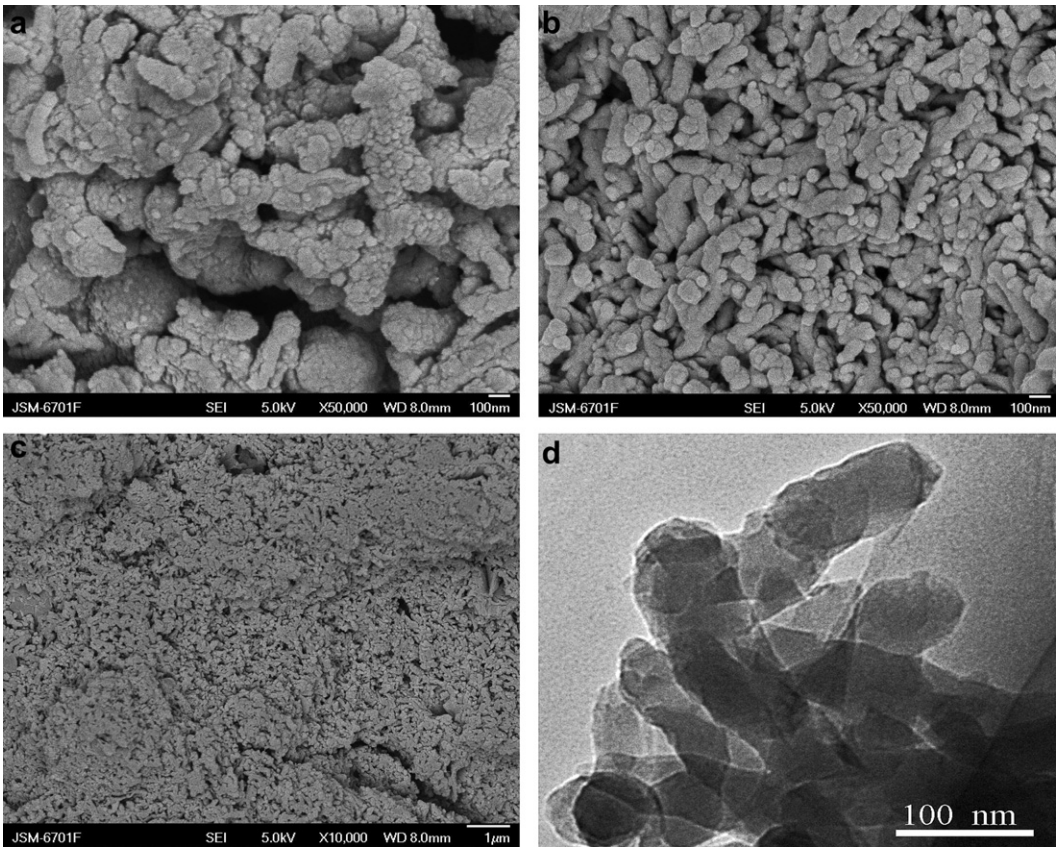

Fig. 1. SEM images of (a) Pure PANI, (b and c) PANI/CMC composites, and (d) TEM image of PANI/CMC composites.

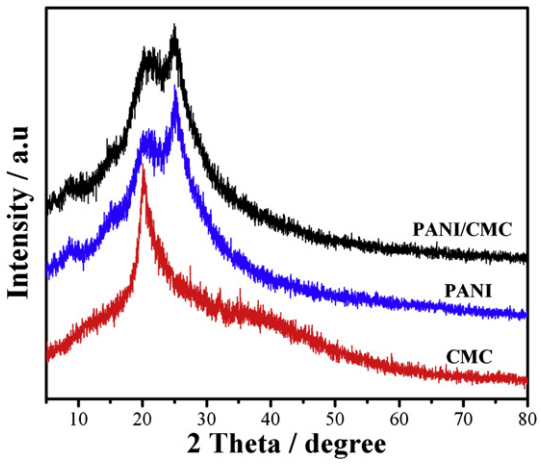

Fig. 2. XRD patterns of CMC, pure PANI, and PANI/CMC composites.

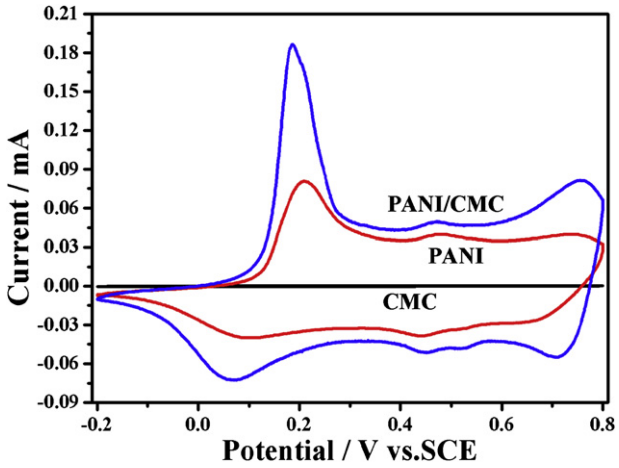

Fig. 4. CV curves of CMC, pure PANI, and PANI/CMC electrodes at a scan rate of 10 mV s^{-1} in 1 M H_2SO_4.

ascribed to the C=C stretching deformation of quinoid and benzene rings, respectively, 1304 and 1249 cm^{-1} to the C–N and C=N stretching band of an aromatic amine, and 1118 and 795 cm^{-1} to the in-plane and out of plane bending of C–H, respectively [28,29]. PANI/CMC has characteristic peaks of both PANI and CMC, e.g. peaks at 1589 and 1498 cm^{-1} for the characteristic peak of quinoid and benzene rings of pure PANI, and peaks at 2923, 2855 and 1627 cm^{-1} (weak peaks) for aliphatic C–H stretching vibrations and carbonyl stretching vibrations of CMC, respectively. The results confirm that the PANI was successfully attached onto the CMC surface.

3.3. Electrochemical properties

In order to evaluate the electrochemical properties of the CMC, pure PANI and PANI/CMC nanorods, cyclic voltammetry (CV) and galvanostatic charge/discharge tests were performed. The CV curves for the CMC, pure PANI and PANI/CMC nanorod electrodes are presented in Fig. 4 at a scan rate of 10 mV s^{-1} in the potential window of −0.2–0.8 V. The CV curve of the CMC is a horizontal straight line without any redox peaks, which indicates that CMC only possesses a negligible electrical double-layer capacitance. However, the capacitance characteristic of PANI or PANI/CMC is distinct from that of the electric double-layer capacitance and close to the ideal rectangular shape with pseudocapacitance characteristics. PANI or PANI/CMC composite has three pairs of redox peaks: the first couple of peaks (about 0.21 V/0.10 V) are attributed to the redox transition of PANI between a semi-conducting state (leucoemeraldine form) and a conducting state (polaronicemeraldine form); the second couple of peaks (about 0.48 V/0.44 V) are due to the transformation between the *p*-benzoquinone/hydroquinone couple because of the attack by water; the third couple of peaks (about 0.76 V/0.70 V) are due to the formation/reduction of bipolaronic pernigraniline and protonated quinonediimine [20,30,31]. However, the electrochemical performances of PANI/CMC composite are different from the pure PANI. The CV curve area of PANI/CMC is larger than that of pure PANI. Furthermore, the first and the third couples of peaks of PANI/CMC composite are obviously higher than pure PANI at same scan rate in 1 M H_2SO_4, and this verifies that PANI/CMC composite has a higher specific capacitance than pure PANI, because of the linear relation between specific capacitance and CV curve area.

Fig. 5 presents CV curves for the PANI/CMC composite electrodes at various scan rates. CV curve area increases with increasing scan rate. It was reported the pseudocapacitance of PANI is due to the

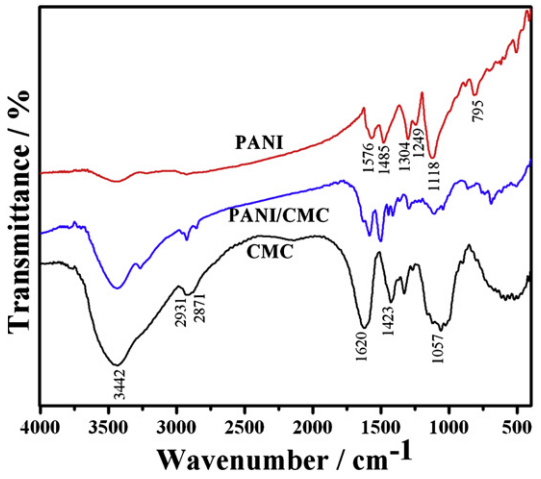

Fig. 3. FT-IR spectra of CMC, pure PANI and PANI/CMC.

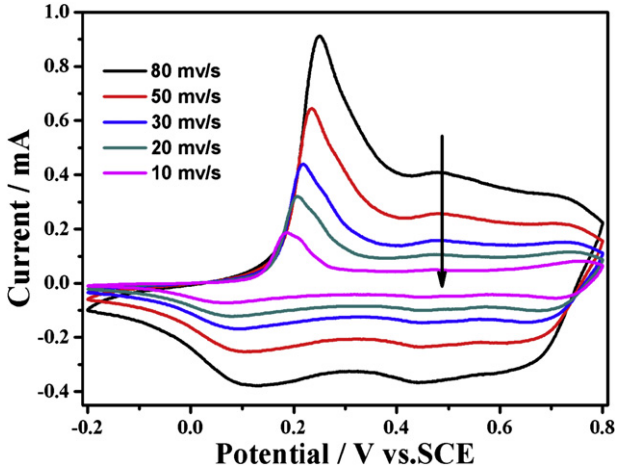

Fig. 5. Cyclic votammograms of a PANI/CMC electrode at various scan rates in 1 M H_2SO_4.

redox reaction involving of the influx and outflow of counter ions from the polymer [15]. Therefore, the CVs of the PANI/CMC composite represent the reversible redox processes. Three pairs of redox peaks are observed in the curve even at scan rates to 80 mV s^{-1}. The first couple of peaks are significantly high, and the third couple of peaks are relatively flat but visible yet. Consequently, the PANI/CMC has a good electrochemical stability.

CV curves for various mass ratios of CMC to aniline are given in Fig. 6. As the CMC content increases to 20 wt%, a maxiumum CV curve area of PANI/CMC is obtained. When the CMC content is 10 wt %, the morphology and size of the PANI don't have a complete change, and agglomeration still appears. Therefore, the electrochemical properties of PANI/CMC are not well presented. However, it is found that the CV curve area of PANI/CMC decreases when the CMC content becomes 30 wt%. The presence of CMC as a polymerization template in the polymerization system can result in the change in the morphology of PANI, and the CMC itself does not contribute to the electrical capability. Therefore, the decrease in the CV curve area is because a large amount of CMC does not involve in the formation of the PANI/CMC particles, and excess of the CMC will prevent the transfer of electrons and gathering the charge. The optimal mass ratio of CMC to aniline monomer for specific capacitance is 0.25.

Fig. 7 gives the galvanostatic charge/discharge curves of pure PANI and PANI/CMC nanorod electrodes at a current density of 1 A g^{-1}. It can be seen that the charge curves are almost linear and symmetrical to their discharge counterparts, indicating good electrochemical performance of the PANI/CMC composites. The specific capacitance of the electrode can be calculated using the following equation [32]

$$C_m = C/m = (It)/(\Delta V\, m) \quad (1)$$

where C_m is specific capacitance (F g^{-1}), I is charge/discharge current (A), t is the time of discharge (S), ΔV is the voltage difference between the upper and lower potential limits, and m is the mass of the active electrode material. According to the above equation, the gravimetric capacitance of PANI/CMC (451.25 F g^{-1}) is much higher than pure PANI (271 F g^{-1}) at a current density of 1 A g^{-1}. This result verifies the effect of CMC on the polymerization as the template, which is in agreement with the result of the CV curves.

The galvanostatic charge/discharge is a reliable method to evaluate the electrochemical capacitance of materials. The Fig. 8a presents the charge/discharge curves of the PANI/CMC composite at various current densities of 1, 2, 3, 5, and 10 A g^{-1}. The discharge capacitances at various current densities are plotted in Fig. 8b. It is evident that the capacitance of this composite slowly decreases as

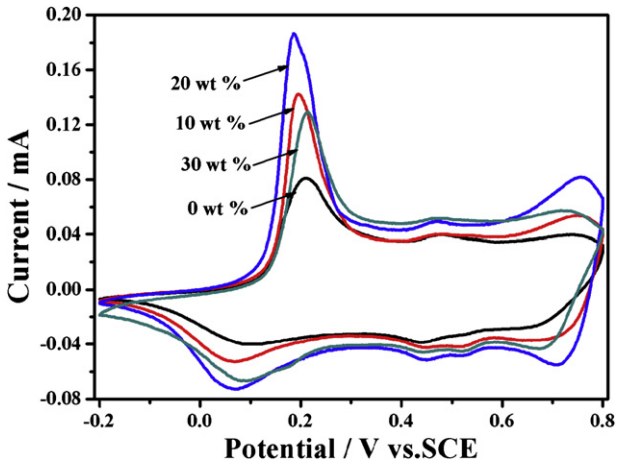

Fig. 6. Cyclic votammograms of a PANI/CMC electrode with different CMC content (wt %) at a scan rate of 10 mV s^{-1} in 1 M H_2SO_4.

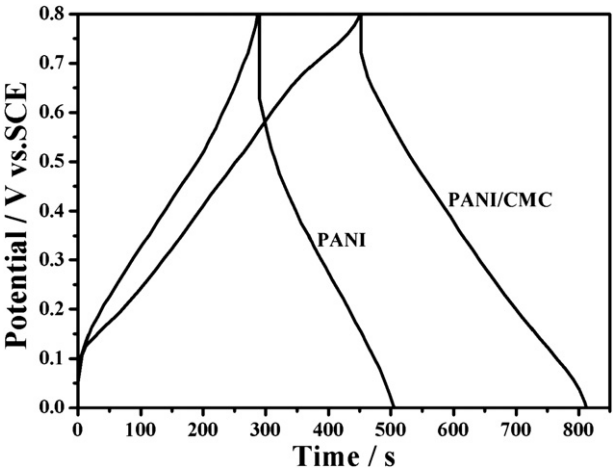

Fig. 7. Galvanostatic charge/discharge curves of pure PANI and PANI/CMC nanorod electrodes at a current density of 1 A g^{-1} in 1 M H_2SO_4.

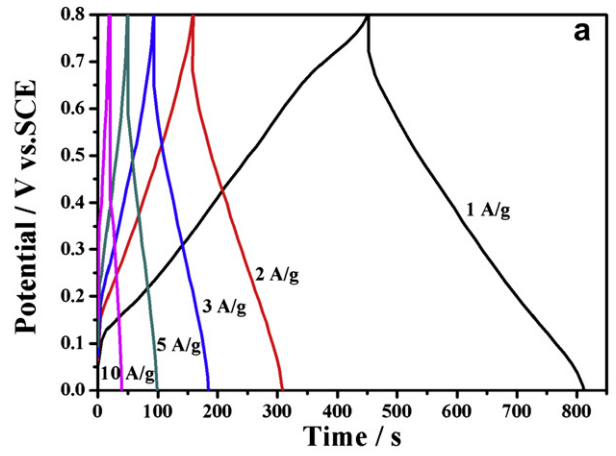

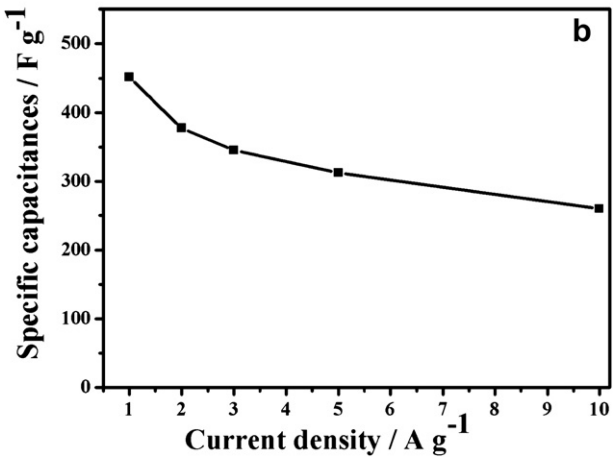

Fig. 8. (a) Galvanostatic charge/discharge curves of PANI/CMC nanorod electrodes at various current densities; (b) Discharge capacitances at various current densities in 1 M H_2SO_4.

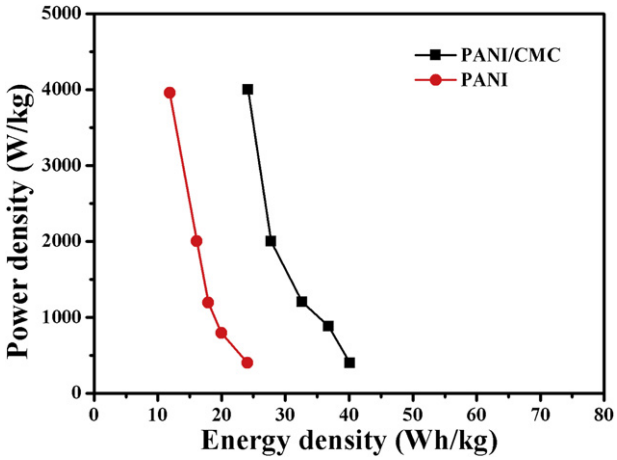

Fig. 9. Ragone plots of pure PANI and PANI/CMC composite.

the current density becomes larger. The result indicates the high capacitance of PANI/CMC composite can be maintained under high current density and it has better rate capability than pure PANI.

The Ragone plots for the pure PANI and PANI/CMC composite are shown in Fig. 9. The specific energy density (E) and power density (P) are evaluated according to equations [33]:

$$E = (1/2)CV^2 \quad (2)$$

$$P = E/\Delta t \quad (3)$$

where C is the capacitance of the two-electrode capacitor, V is the voltage decrease in discharge, E is the energy and Δt is the time spent in discharge. As seen from the Ragone plots, as the power density increases from 399 W/kg to 3961 W/kg, the energy density of pure PANI decreases from 24.1 Wh/kg to 11.8 Wh/kg. Comparatively, the energy density of the PANI/CMC composite can reach 40.1 Wh/kg at a power density of 401 W/kg, and still remains 24.1 Wh/kg at a power density of 4000 W/kg, which exhibited a large power range that can be obtained while maintaining a relatively high energy density. The results illustrate that the PANI/CMC composite materials have excellent electrochemical properties of high energy density and power output.

The cycling stability of PANI and PANI/CMC electrodes was measured by charge/discharge cycling at a current density of 1 A g^{-1}, as shown in Fig. 10. The specific capacitance of pure PANI remains only 28% after 1000 charge/discharge cycles. However, the PANI/CMC electrode shows a slight decrease and its capacitance remains greater than 300 F g^{-1} after 1000 cycles. This result demonstrates that the improved cycling stability is due to the intermolecular interaction between the PANI chains and the CMC template, and it restricts the change of the nanostructure. Therefore, the PANI/CMC nanorod exhibits an excellent cycling stability.

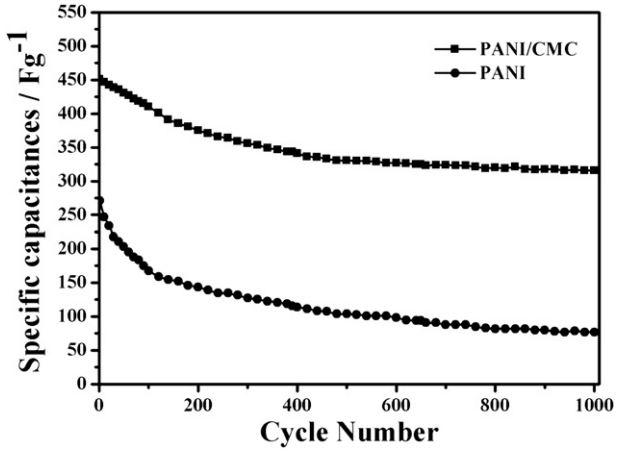

Fig. 10. Variations of the specific capacitances of pure PANI and PANI/CMC composite electrodes as a function of cycle number measured at the charge/discharge current density of 1 A g^{-1}.

4. Conclusions

PANI/CMC nanorods with uniform diameters about 100 nm were synthesized via one-step in-situ oxidation polymerization of aniline using rod-like sodium carboxymethyl cellulose as a polymerization oriented agent. The maximum value of specific capacitance reaches 451.25 F g^{-1}, and the capacitance retention remains higher than 300 F g^{-1} after 1000 cycles. These results suggest that the electrodes made of PANI/CMC nanorods could have an excellent specific capacitance and good rate capability at large current densities.

Acknowledgements

We thank to the National Natural Science Foundation of China (NO.21164009), the program for Changjiang Scholars and Innovative Research Team in University (IRT1177), Key Laboratory of Eco-Environment-Related Polymer Materials (Northwest Normal University) of Ministry of Education, and Key Laboratory of Polymer Materials of Gansu Province.

References

[1] M. Winter, R.J. Brodd, Chem. Rev. 104 (2004) 4245–4269.
[2] L.L. Zhang, X.S. Zhao, Chem. Soc. Rev. 38 (2009) 2520–2531.
[3] D.D. Zhao, S.J. Bao, W.J. Zhou, H.L. Li, Electrochem. Commun. 9 (2007) 869–874.
[4] T. Zhu, J.S. Chen, X.W. Lou, J. Mater. Chem. 20 (2010) 7015–7020.
[5] W. Sugimoto, H. Iwata, Y. Yasunaga, Y. Murakami, Y. Takasu, Angew. Chem. Int. Ed. 42 (2003) 4092–4096.
[6] S. Ghosh, O. Inganäs, Adv. Mater. 11 (1999) 1214–1218.
[7] C.J. Yu, C. Masarapu, J.P. Rong, B.Q. Wei, Adv. Mater. 21 (2009) 4793–4797.
[8] C.G. Liu, Z.N. Yu, D. Neff, A. Zhamu, B.Z. Jang, Nano Lett. 10 (2010) 4863–4868.
[9] C.Q. Bian, A.S. Yu, H.Q. Wu, Electrochem. Commun. 11 (2009) 266–269.
[10] T.C. Girija, M.V. Sangaranarayanan, J. Power Sourc. 159 (2006) 1519–1526.
[11] F. Montilla, M.A. Cotarelo, E. Morallon, J. Mater. Chem. 19 (2009) 305–310.
[12] Z. Lei, H. Zhang, S. Ma, Y. Ke, J. Li, F. Li, Chem. Commun. 7 (2002) 676–677.
[13] Y.F. Yan, Q.L. Cheng, G.C. Wang, C.Z. Li, J. Power Sourc. 196 (2011) 7835–7840.
[14] K. Lota, V. Khomenko, E. Frackowiak, J. Phys. Chem. Solids 65 (2004) 295–301.
[15] S.H. Mujawar, S.H. Lee, Electrochim. Acta 56 (2011) 4462–4466.
[16] X.M. Feng, R.M. Li, Y.M. Ma, R.F. Chen, Adv. Funct. Mater. 21 (2011) 2989–2996.
[17] G.A. Snook, P. Kao, A.S. Best, J. Power Sourc. 196 (2011) 1–12.
[18] S.X. Xing, Y. Chu, X.M. Sui, Z.S. Wu, J. Mater. Sci. 40 (2005) 215–218.
[19] D.H. Zhou, Y.H. Li, J.Y. Wang, P. Xu, X.J. Han, Mater. Lett. 65 (2011) 3601–3604.
[20] Y.Z. Li, X. Zhao, Q.H. Zhang, Langmuir 27 (2011) 6458–6463.
[21] A.P. Rokhade, S.A. Agnihotri, S.A. Patil, N.N. Mallikarjuna, P.V. Kulkarni, T.M. Aminabhavi, Carbohydr. Polym. 65 (2006) 243–252.
[22] S. Magdassi, A. Bassa, Y. Vinetsky, A. Kamyshny, Chem. Mater. 15 (2003) 2208–2217.
[23] J. Li, H.M. Dahn, L.J. Krause, D.B. Le, J.R. Dahn, J. Electrochem. Soc. 155 (2008) 812–816.
[24] F. He, D.Y. Zhao, J.C. Liu, C.B. Roberts, Ind. Eng. Chem. Res. 46 (2007) 29–34.
[25] Z.M. Zhang, Z.X. Wei, M.X. Wan, Macromolecules 35 (2002) 5937–5942.
[26] J.P. Pouget, M.E. Jozefowicz, A.J. Epstein, X. Tang, A.G. MacDiarmid, Macromolecules 24 (1991) 779–789.
[27] Q.T. Qu, S.B. Yang, X.L. Feng, Adv. Mater. 23 (2011) 5574–5580.
[28] A.P. Monkman, P. Adams, Synth. Met. 41 (1991) 87–96.
[29] S.X. Xing, C. Zhao, S.Y. Jing, Z.C. Wang, Polymer 47 (2006) 2305–2313.
[30] C.H. Hu, C.H. Chu, J. Electroanal. Chem. 503 (2001) 105–116.
[31] C.H. Hu, J.Y. Lin, Electrochim. Acta 47 (2002) 4055–4067.
[32] A.L.M. Reddy, S. Ramaprabhu, J. Phys. Chem. C 111 (2007) 7727–7734.
[33] W. Xing, S.Z. Qiao, R.G. Ding, F. Li, G.Q. Lu, Z.F. Yan, H.M. Cheng, Carbon 44 (2006) 216–224.